Chemical Oxidative Polymerization of Safranines

Gordana Ćirić-Marjanović,*,† Natalia V. Blinova,‡ Miroslava Trchová,‡ and Jaroslav Stejskal‡

Faculty of Physical Chemistry, University of Belgrade, Studentski trg 12-16, 11001 Belgrade, Serbia, and Institute of Macromolecular Chemistry, Academy of Sciences of the Czech Republic, 162 06 Prague 6, Czech Republic

Received: November 9, 2006; In Final Form: December 28, 2006

Phenosafranine and safranine have been oxidized with ammonium peroxydisulfate in acidic aqueous solution. The oxidative coupling of both safranines was proved by gel permeation chromatography demonstrating the presence of oligomeric chains of mass-average molar masses 6500 and 4500 g mol^{-1} for polyphenosafranine and polysafranine, respectively. A theoretical study of the mechanism of safranine and phenosafranine polymerization was based on the MNDO-PM3 semiempirical quantum chemical computations of the heat of formation of dimeric reaction intermediates, taking into account solvation effects. The study of the redox properties of the hydrated safranines and their reactive species shows that nitrenium cations are the main reactive species generated by the oxidation of the parent safranines with a two-electron oxidant, peroxydisulfate, in the initiation phase. The dominant dimers of safranines are formed by N−C coupling reactions between nitrenium cations and the parent safranines. The main coupling reactions of phenosafranine are N−C2 (C8) and N−C4 (C6); N−C4 (C6) is the dominant coupling mode for safranine. The molecular structure of oligosafranines has been studied by FTIR, Raman, and UV−vis spectroscopies. Besides prevalent unoxidized monomeric units, polymerization products of safranines contain also the iminoquinonoid and newly formed fused phenazine units.

Introduction

The creation of polymers by the oxidative polymerization of aromatic diamines is one of the latest advances in the field of conducting polymers.[1] Polymers of aromatic diamines, such as phenylenediamines, diaminonaphthalenes, diaminoanthraquinones, benzidine and its derivatives, naphthidine, diaminophenazines, and diaminopyridines have received increasing attention and have been extensively investigated during the past decade. Aromatic diamine monomers are susceptible to oxidative polymerization via oxidation of one or both amino groups to give linear poly(aminoanilines) and poly(aminonaphthylamines), ladder polyphenazines, and polymers containing phenazine units.

Aromatic diamine polymers have novel functions in comparison with the common conducting polymers, polyaniline and polypyrrole. They include tunable electroactivity,[2] high permselectivity to various electroactive species,[3] unique electrochromism,[4] linear sensitivity of the conductivity to moisture,[5] controlled variation in the conductivity with temperature[6] and external electric field,[7] high sensibilities of the polymer-modified electrodes to biosubstances at an extremely low concentration,[8] good ability in detecting electroinactive anions,[9] pronounced electrocatalytic properties,[10] effective absorption of heavy-metal ions,[11] anticorrosion ability, strong adhesion to metals,[12,13] and high capacitance.[14]

Diaminophenazines are monomers of particular theoretical and practical interest because they already contain a phenazine ring, shown to be an important redox structural unit of a number of aromatic diamine polymers formed in the course of oxidative polymerization.[1,15] An electrochemical, spectroscopic, and theoretical study of poly(2,3-diaminophenazine) by Thomas and Euler[16] suggested that the structural differences between poly-

SCHEME 1: Phenosafranine and Safranine

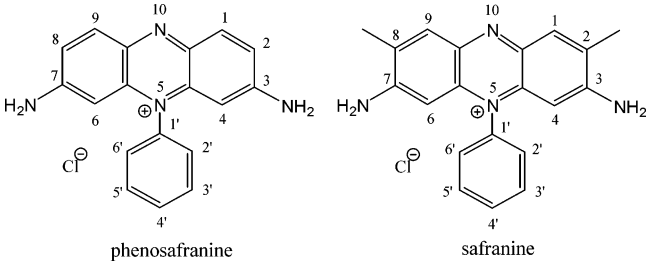

(2,3-diaminophenazine) and the related poly(*o*-phenylenediamine) arise from different coupling positions between monomer units during polymerization. Visible reflectance spectra recorded for these two polymers also indicate that poly(*o*-phenylenediamine) contains quinonediimine linkages not found in poly(2,3-diaminophenazine).

Safranine dyes, phenosafranine (3,7-diamino-5-phenylphenazinium chloride) and safranine (3,7-diamino-2,8-dimethyl-5-phenylphenazinium chloride; Safranin T, Basic Red 2) are well-known diaminophenazine derivatives (Scheme 1). Phenosafranine has been electropolymerized by several research groups.[17−21] The redox properties of polyphenosafranine (PPSF) were investigated at its different oxidation and protonation levels by potential scan voltammetry and electrochemical impedance spectroscopy.[17] It has been shown that the polymer contains phenosafranine units linked by secondary amino groups. A two-electron, two-proton process was proposed as the main redox reaction; the reduction yields the corresponding 5-hydrophenazine form. The polymers resembled redox polymers rather than conducting polymers. The electrocatalytic effect of PPSF films on the oxidation of 1,1′-ferrocenedimethanol,[18] as well as on the oxidation of reduced β-nicotinamide adenine dinucleotide,[19] was described. The oxidation of phenosafranine at a glassy

† Faculty of Physical Chemistry.
‡ Institute of Macromolecular Chemistry.

10.1021/jp067407w CCC: $37.00
Published on Web 02/10/2007

carbon electrode gives rise to a stable redox-active electropolymerized PPSF film.[20] The film exhibited potent and persistent electron-mediating behavior followed by the well-separated oxidation peaks toward ascorbic acid, dopamine, and serotonin. Simultaneous determination of these compounds at the PPSF electrode was performed. The mediated reduction of oxygen at a PPSF electrode has also been studied.[21]

The single-electron oxidation of safranine by specific oxidizing radicals has been investigated by using the nanosecond-pulse radiolysis technique.[22] The semi-oxidized safranine species formed by these reactions have been shown to exist in two acid−base forms with $pK_a = 4.0$. Oxidation of safranine in aqueous solution using Fenton's reagent[23] or dichromate in dilute sulfuric acid in the presence of oxalic acid[24] was also investigated. Characterization of safranine-based thin-film sandwich devices by analyzing their electrical and photoelectrical behavior revealed that safranine behaves as a semiconductor.[25] A redox polymer containing safranine has been prepared.[26] Polysafranine (PSF) dye was used as a leveling component, improving the quality of electrodeposited copper coatings.[27] Safranine was used in the synthesis of a new generation of polymers with intrinsic fluorescence, poly(Schiff bases)-bifluorophores.[28]

Our recent studies have indicated the formation of safranine-like structures, containing *N*-phenylphenazinium rings, as intermediates in the chemical oxidative polymerization of aniline.[29] It has been proposed that substituted phenazine units may play a fundamental role in the self-assembly of polyaniline to nanotubes and related nanostructures.[30] As in the case of most of the polymers of aromatic diamines, which have been prepared mainly by electrochemical polymerization,[1] there is no report relating to the chemical oxidative preparation of polysafranines. The objectives of the present work are syntheses of safranine and phenosafranine polymers in aqueous solution by the standard chemical oxidative polymerization route, characterization of polymers by a variety of techniques, and elucidation of the polymerization mechanism using the semiempirical MNDO-PM3 quantum chemical computational method. The main structural features of polysafranines revealed by FTIR and Raman spectroscopies are correlated with the dominant dimeric structures proposed on the basis of semiempirical quantum chemical calculations.

Experimental Section

Oxidation of Safranines. Phenosafranine and safranine (0.2 M; Fluka, Switzerland) were oxidized with ammonium peroxydisulfate (0.5 M; Lachema, Czech Republic) in 0.2 M hydrochloric acid. The oxidant solution was poured into the monomer solution at 20 °C, and the reaction mixture was left for 24 h. The original red solution converted to a dark red precipitate suspended in colorless aqueous medium. The solids were collected on a filter, rinsed with 0.2 M hydrochloric acid, and dried in air.

Computational Methods. The semiempirical MNDO-PM3 model[31−33] (included in Molecular Orbital Package[34] MOPAC 97, part of the Chem3D Pro 5.0 package, CambridgeSoft Corporation), with full geometry optimization, has been used to obtain the molecular orbitals, ionization energy, heat of formation, charge distribution (Mulliken charges), and spin density of individual species. Input files for the semiempirical computations were the most stable conformers of the investigated molecular structures, with minimized steric energy using the MM2 molecular mechanics force-field method.[35] The conductor-like screening model (COSMO) technique was used to approximate the effect of a solvent model surrounding the molecule.[36] The restricted Hartree−Fock method has been used for the molecular structures and the unrestricted Hartree−Fock method for radical species.

TABLE 1: Properties of Polysafranines Prepared by the Oxidation of Phenosafranine or Safranine in Aqueous Medium

property	oxidation product[a] of phenosafranine	oxidation product[a] of safranine
yield, %	82	93
conductivity,[b] S cm^{-1}	3.7×10^{-10}	6.2×10^{-10}
density,[c] g cm^{-3}	1.39	1.34
molecular weight,[d] M_w	6500	4500
polydispersity,[d] M_w/M_n	5.8	5.3
soluble in	*N*-methylpyrrolidone, dimethylsulfoxide	
color	dark red	

[a] Safranine (0.2 M) was oxidized with ammonium peroxydisulfate (0.5 M) in 0.2 M hydrochloric acid. [b] By two-probe method after deposition of gold electrodes on fronts of compressed samples. [c] By Archimedes method, i.e., by weighing the samples in air and immersed in decane. [d] M_w and M_n are the weight- and number-averages of molecular weight, respectively, obtained by gel permeation chromatography in *N*-methylpyrrolidone.

Spectroscopic Characterization. IR spectra of the samples dispersed in potassium bromide were recorded at 2 cm^{-1} resolution with a Thermo Nicolet NEXUS 870 FTIR spectrometer with a DTGS TEC detector. Raman spectra excited by a 633 nm HeNe laser were collected with a Renishaw inVia Reflex Raman microscope, using a 50× objective to focus the laser beam on the sample placed on a $X-Y$ motorized stage. The scattered light was analyzed by a spectrograph with a holographic grating (1800 lines mm^{-1}). A Peltier-cooled CCD detector (578 × 385 pixels) registered the dispersed light. The UV−vis absorption spectra of the samples dissolved in *N*-methylpyrrolidone were determined with a Hewlett-Packard 8451 spectrophotometer.

Gel Permeation Chromatography. Molecular weights were assessed with a GPC/SEC apparatus using a 8 × 600 mm PLMixedB column (Polymer Laboratories, U.K.) operating with *N*-methylpyrrolidone and calibrated with polystyrene standards with spectrophotometric detection at 650 nm. The samples were dissolved in *N*-methylpyrrolidone containing 0.025 g cm^{-3} triethanolamine for deprotonation of samples and 0.005 g cm^{-3} lithium bromide to prevent aggregation.

Results and Discussion

Properties of Polysafranines. The red solutions of soluble safranines turn to a dark red precipitate suspended in a colorless medium after the addition of an oxidant. This fact is an indication that the coupling of safranine molecules to chains took place. The oxidation products of safranines are discussed in the present paper as polymers, although, in fact, they are rather oligomers. Their molar masses are of the order of thousands (Table 1), and the average number of constitutional units in such polysafranines is about 20.

Because of the close relation to the reaction intermediates in the oxidation of aniline, yielding the conducting polymer, polyaniline,[37] the potential conductivity is a property of interest. Both oxidation products of safranines, however, are nonconducting, having a conductivity of the order 10^{-10} S cm^{-1} (Table 1), i.e., close to the conductivity of the polyaniline base.[37]

Theoretical Approach to the Oxidative Polymerization of Safranines. The classical structural formulas of safranine and phenosafranine are somewhat misleading, treating them exclusively as aromatic diamines (Scheme 1). In fact, both safranines

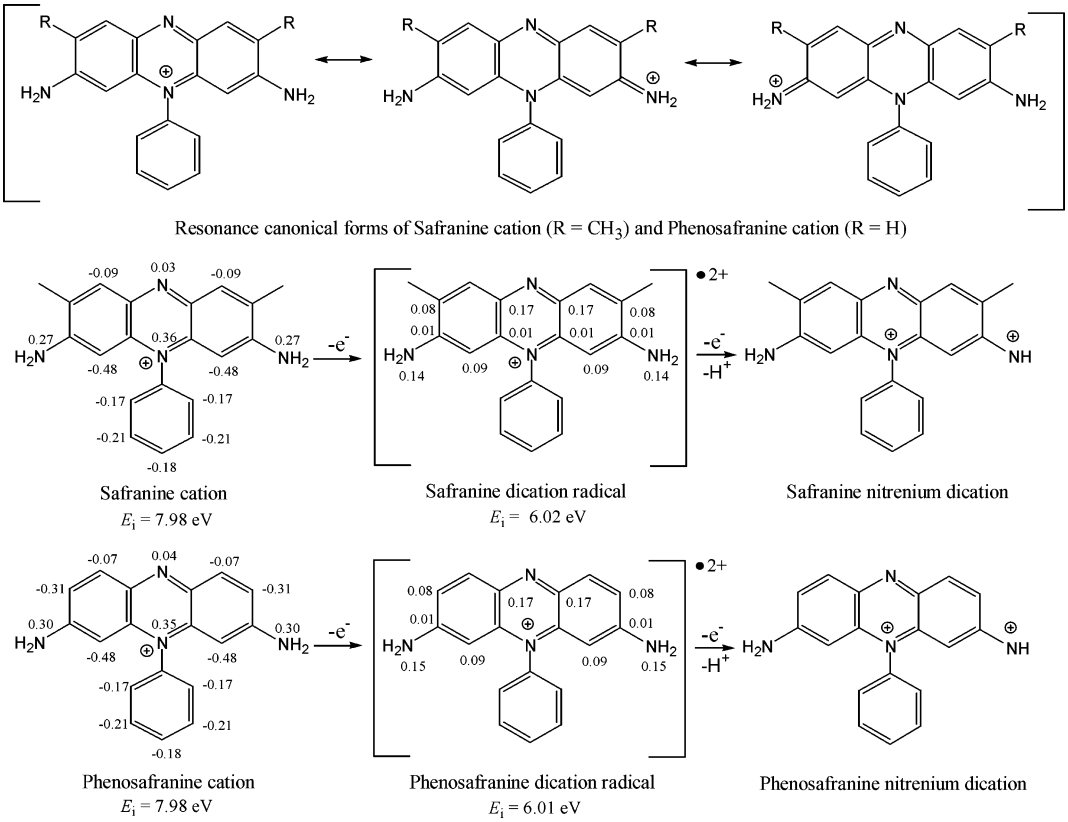

Figure 1. Generation of dication radicals and nitrenium dications of phenosafranine and safranine. Charge distribution of hydrated safranines cations, spin density of their hydrated dication radicals, and E_i of these species, calculated by the PM3 method, are shown.

have a partial iminoquinonoid character (Figure 1), similar to aniline black. This was confirmed by the PM3-computed charge distribution of safranine cations (Figure 1), showing substantial delocalization of positive charge over three nitrogen atoms (both amino as well as phenyl-substituted nitrogens). The ionization energies (E_i) of the phenosafranine cation, the safranine cation, and their dication radicals, calculated by the PM3 method, indicate that the dication radicals of both safranines are more oxidizable than the parent safranine cations in aqueous solution (Figure 1). It follows that the generation of hydrated safranine dication radicals as stronger reductants in comparison with hydrated safranines cations, and of the sulfate anion radical as a stronger oxidant (2.5−3.1 V vs NHE)[38] than the peroxydisulfate anion (2.0−2.1 V vs NHE),[39] represents an unfavored initiation reaction in the oxidation of safranines with the two-electron oxidant, peroxydisulfate:

$$[\text{Safranine}]^+-\text{NH}_2 + \text{S}_2\text{O}_8^{2-} \rightarrow [\text{Safranine}]^+-\text{NH}_2^{+\bullet} + \text{SO}_4^{-\bullet} + \text{SO}_4^{2-} \quad (1)$$

It is proposed that the oxidation proceeds further to the generation of safranine nitrenium dications as reactive species:

$$[\text{Safranine}]^+-\text{NH}_2 + \text{S}_2\text{O}_8^{2-} \rightarrow [\text{Safranine}]^+-\text{NH}^+ + \text{SO}_4^{2-} + \text{HSO}_4^- \quad (2)$$

The initiation process could be complicated by the presence of chlorides in the reaction solution:

$$\text{Cl}^- + \text{S}_2\text{O}_8^{2-} \rightarrow \text{Cl}^\bullet + \text{SO}_4^{-\bullet} + \text{SO}_4^{2-} \quad (3)$$

$$\text{Cl}^- + \text{Cl}^\bullet \rightarrow \text{Cl}_2^{-\bullet} \quad (4)$$

Thus formed chlorine anion radicals and sulfate anion radicals, both strong one-electron oxidants, can further oxidize safranines, thus generating their dication radicals:

$$[\text{Safranine}]^+-\text{NH}_2 + \text{Cl}_2^{-\bullet} \rightarrow [\text{Safranine}]^+-\text{NH}_2^{+\bullet} + 2\text{Cl}^- \quad (5)$$

$$[\text{Safranine}]^+-\text{NH}_2 + \text{SO}_4^{-\bullet} \rightarrow [\text{Safranine}]^+-\text{NH}_2^{+\bullet} + \text{SO}_4^{2-} \quad (6)$$

Because hydrated safranine cations are much more oxidizable ($E_i \sim 8.0$ eV) than hydrated chloride anions ($E_i \sim 12.1$ eV), it is assumed that nitrenium dications are the dominant reactive species generated in the initiation phase. However, the existence of safranine dication radicals cannot be neglected.

The generated safranine nitrenium dications, being strong electrophiles, instantaneously react with surrounding safranine molecules leading to the formation of dimeric trication intermediates, further being transformed to the safranine dimers by releasing protons (Figure 2). Charge distribution calculations of phenosafranine and safranine cations (Figure 1) indicate that the C2 (C8) and C4 (C6) atoms of the phenazine ring of the phenosafranine, and the C4 (C6) atoms of the phenazine ring of the safranine, are the main reactive centers for electrophilic nitrenium dication attack, characteristic of the chemical oxidative polymerizations of aromatic amines via the electrophilic aromatic substitution reaction pathway. According to the Hammond postulate,[40] the reaction of the safranine nitrenium dication with the safranine cation is governed not by the stability of the final dimeric products but by the stability of the safranine dimer trication intermediate, resembling structurally the transition state, as nearest to it on the reaction path. On the basis of the MNDO-

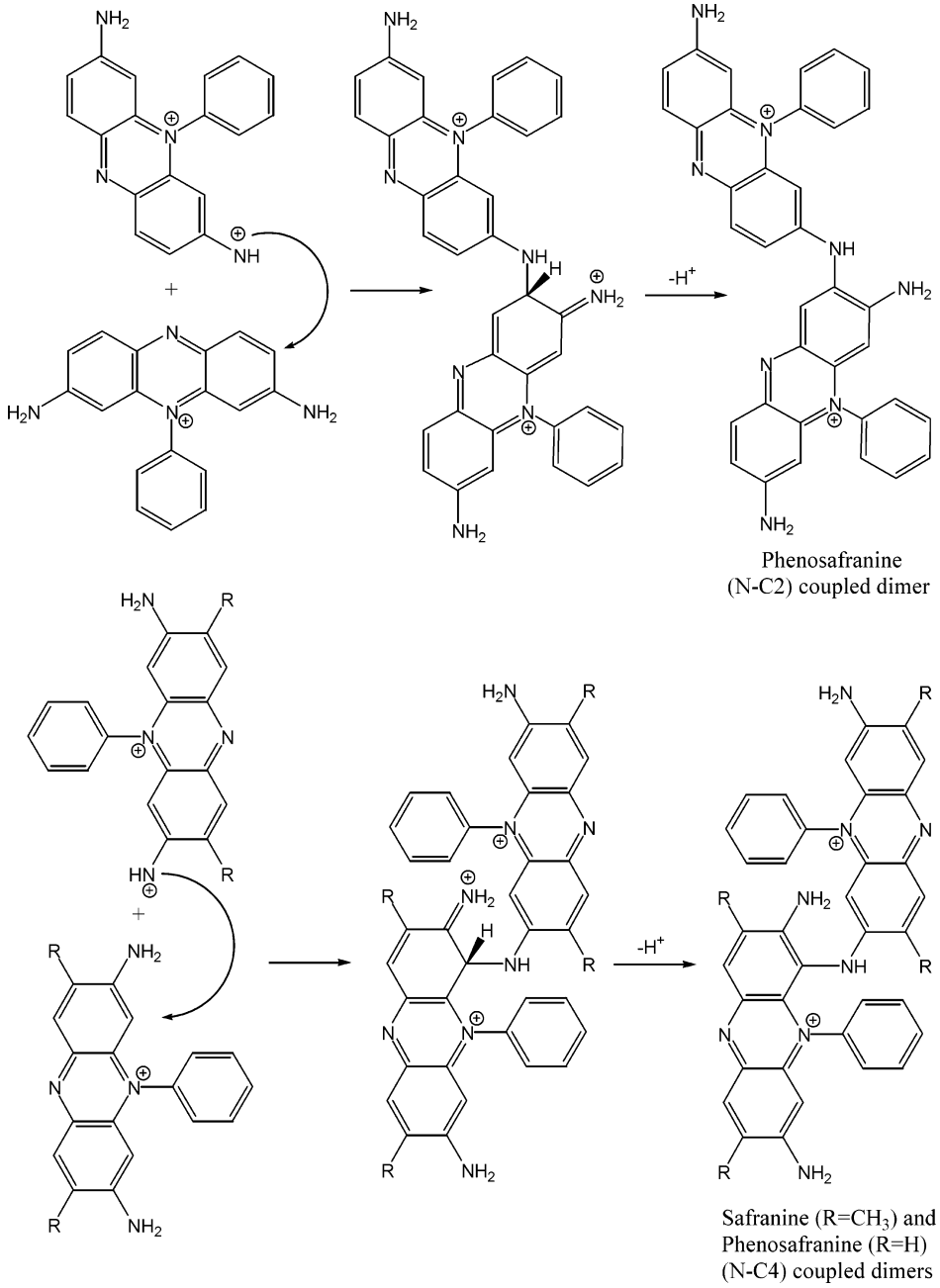

Figure 2. The main safranine dimers obtained by the deprotonation of the most stable dimeric trication intermediates, formed by the reaction of the safranine cations with their nitrenium dication reactive species.

TABLE 2: Heat of Formation, ΔH_f, for Hydrated Safranine and Phenosafranine Dimer Trication Intermediates, Calculated by PM3 Method

coupling mode (nitrenium dication + parent cation)	ΔH_f (kcal mol^{-1})	
	safranine	phenosafranine
N−C1(C9)	530.4	558.0
N−C2(C8)	−[a]	525.0
N−C4(C6)	499.8	522.5
N−C2′(C6′)	530.5	558.9
N−C3′(C5′)	530.9	558.0
N−C4′	518.0	545.9
N−N	517.2	545.7

[a] Data not available.

PM3 computations of the heat of formation (ΔH_f) of the safranine trication intermediates (Table 2), it has been concluded that the main coupling reactions of phenosafranine are N−C2 (C8) and N−C4 (C6); N−C4 (C6) is the dominant coupling mode for safranine (Figure 2). We came to the same conclusions concerning the coupling reactions of safranines after similar considerations of the above-mentioned possible side reaction of the safranines with their dication radical species. On the basis of calculated ΔH_f values of safranine and phenosafranine dimer intermediates (presented in Table 2), it can be concluded that the N−N coupling reaction of both safranines is much less probable because the ΔH_f of the safranine dimer intermediate formed by N−N coupling (517.2 kcal mol^{-1}) is significantly higher than the ΔH_f of the safranine dimer intermediate formed by the dominant coupling mode N−C4(C6) (499.8 kcal mol^{-1}), and the ΔH_f of the phenosafranine dimer intermediate formed by N−N coupling (545.7 kcal mol^{-1}) is significantly higher than the ΔH_f of the phenosafranine dimer intermediates formed by the dominant coupling modes N−C4(C6) (522.5 kcal mol^{-1}) and N−C2(C8) (525.0 kcal mol^{-1}).

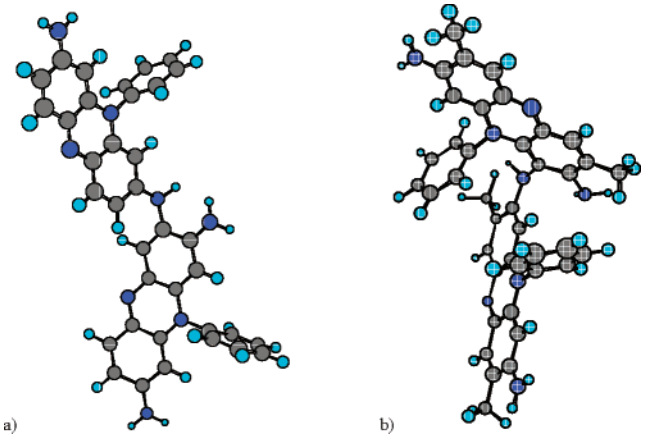

Figure 3. The most stable conformations of the (a) phenosafranine N−C2 coupled dimer and (b) safranine N−C4 coupled dimer.

The main dimers of safranines have twisted structures (Figure 3). Internal steric repulsions are much more pronounced for the safranine N−C4 coupled dimer, causing an almost perpendicular position of two monomeric structural units. All the phenyl rings are twisted out of the phenazine ring planes by almost 90°. It follows that the existence of delocalized polarons is possible only for oligophenosafranine; in the case of oligosafranine, only isolated polarons (cation radicals) could be expected.

Safranines dimers (**1, 9**) can be further oxidized to various products (Figures 4 and 5). The heats of formation of the oxidation products indicate that thermodynamic stability increases from the unstable N−C4 phenazinediiminoquinonoid dimer (**6**) (ΔH_f = 519.6 kcal mol^{-1}) to the most stable N−C4 hydrolyzed *ortho*-iminoquinonoid dimer form (**5**) (ΔH_f = 368.7 kcal mol^{-1}) of safranine (Figure 4) and from the unstable N−C2 phenazinediiminoquinonoid dimer (**14**) (ΔH_f = 549.2 kcal mol^{-1}) to the most stable N−C2 hydrolyzed *ortho*-iminoquinonoid dimer form (**13**) (ΔH_f = 400.7 kcal mol^{-1}) of phenosafranine (Figure 5).

Two-electron oxidation of the phenosafranine N−C2 and N−C4 dimers and the safranine N−C4 dimer, followed by intramolecular cyclization, lead to the formation of dihydrophenazine-like structures (**2**, Figure 4; **10**, Figure 5) being easily oxidized further to phenazine-like structures (**4**, Figure 4; **12**, Figure 5). Our computational results suggest that intramolecular cyclization is thermodynamically favorable, because it leads to the formation of a more stable dihydrophenazine-containing dimer [ΔH_f = 387.5 kcal mol^{-1} (**2,** Figure 4) and 402.2 kcal mol^{-1} (**10**, Figure 5)] than the corresponding non-cyclized *ortho*-iminoquinonoid dimer [ΔH_f = 419.3 kcal mol^{-1} (**3**, Figure 4) and 451.9 kcal mol^{-1} (**11**, Figure 5)]; both compared species bearing the same oxidation state. It seems that formation of ladder segments during the course of oxidative polymerization of safranines, characteristic of a number of aromatic diamine polymer growth mechanisms,[1] could be expected.

FTIR Spectroscopy. *Polyphenosafranine.* The FTIR spectra of the phenosafranine monomer and the PPSF base and salt forms are presented in Figure 6. Main absorption bands and their assignments are given in Table 3. The strong and very strong bands due to C═C aromatic ring-stretching vibrations[17,41,42] are observed at 1602, 1533, and 1485 cm^{-1} in the FTIR spectrum of phenosafranine, at 1601, 1521, and 1488 cm^{-1} in the spectrum of the PPSF salt form, as well as at 1602, 1531, and 1487 cm^{-1} in the spectrum of the PPSF base form.

The most notable spectral difference between PPSF and phenosafranine is the appearance of new bands at 1445 (very strong) and 1506 (salt form)/1512 cm^{-1} (base form) (strong) in the spectrum of PPSF, which are not present in the spectrum of phenosafranine and have not been reported for electrochemically synthesized PPSF.[17] These bands suggest the formation of a new aromatic system in the polymeric chains, which is not present in the monomer, and are attributable to the ring-stretching vibrations in a newly formed phenazine segment.[41−43] Such a segment could be formed by the oxidation of two N−C linked phenosafranine units, followed by an intramolecular cyclization reaction (Figure 5). This process can be also regarded as the formation of one pyrazine ring between two adjacent phenosafranine units, leading to ladder segments. The band at 1630 cm^{-1} in the spectra of PPSF is associated with the stretching vibrations of C═N bonds in phenosafranine, newly formed phenazine, and oxidized iminoquinonoid units[17,41,42] and has been attributed also to the C═C stretching vibration in the phenazine rings.[43,44] This band is red-shifted compared with the 1643 cm^{-1} band observed in the spectrum of the phenosafranine monomer. New bands observed at 1694 and 1706 cm^{-1} in the spectra of the PPSF base and salt, respectively, originate from the C═O group stretching.[42] Such a group can be formed by the hydrolysis of imine C═N bonds.

The bands found at 1379, 1377, and 1388 cm^{-1} in the spectra of the monomer, PPSF base and salt, respectively, could be due to the substituted phenazine ring-stretching mode.[43] Li et al.[44] ascribed the band at 1384 cm^{-1} to C−N stretching in the aromatic phenazine ring. The strong absorption peak due to C−N stretching vibrations observed at 1320 cm^{-1} in the spectrum of phenosafranine is shifted to 1313 cm^{-1} in the spectra of the base and salt forms of PPSF.[17,41,45,46] A new shoulder, attributable to C−N stretching, is observed at 1292 cm^{-1} in the spectrum of the PPSF salt. Two very strong bands due to aromatic C−H in-plane deformation vibrations,[42] δ(C−H), are found at 1186 and ∼1132 cm^{-1} in PPSF spectra. The band located at 1186 cm^{-1} is relatively less intense than the band at 1189 cm^{-1} in the monomer spectrum, indicating a change in the substitution pattern on phenosafranine aromatic rings during the polymerization.

The monosubstituted benzene ring in the phenosafranine unit is recognized in the spectrum of the monomer by the bands at 1072, 749, 696, and 607 cm^{-1} (Table 3).[42,45−47] These bands remain almost unchanged in the PPSF spectra, indicating that the polymerization does not proceed via the monosubstituted ring of the monomer.

The intensity of the ∼870 cm^{-1} band has significantly decreased in the spectra of both forms of PPSF compared with that observed for the monomer. For the phenosafranine monomer, this band is assigned to γ(C−H) vibration of 1,2,4-trisubstituted fused benzene ring (one isolated H atom).[42,45,46] Weakening of this band suggests transformation of the 1,2,4-trisubstituted to tetrasubstituted patterns (1,2,4,5- and 1,2,3,4-) on phenosafranine fused benzene rings during the polymerization process. The new bands at 926 and ∼882 cm^{-1} in the spectra of polymeric samples, due to γ(C−H) vibrations of a lone H atom,[42,45,46] correspond to a newly formed 1,2,4,5-tetrasubstituted patterns on phenosafranine fused benzene rings in the polymer. The monomer bands at 973 and 830 cm^{-1} due to the aromatic δ(C−H) mode, and the γ(C−H) vibration for two adjacent H atoms in the 1,2,4-trisubstituted ring,[46] respectively, are still present in the spectra of PPSF at the similar positions, indicating the preservation of such rings in the polymeric chains. This means that PPSF contains both ring-opened and ladder segments.

In the high frequency IR region, the monomer spectrum shows bands at 3443 and ∼3379 cm^{-1}, corresponding to the

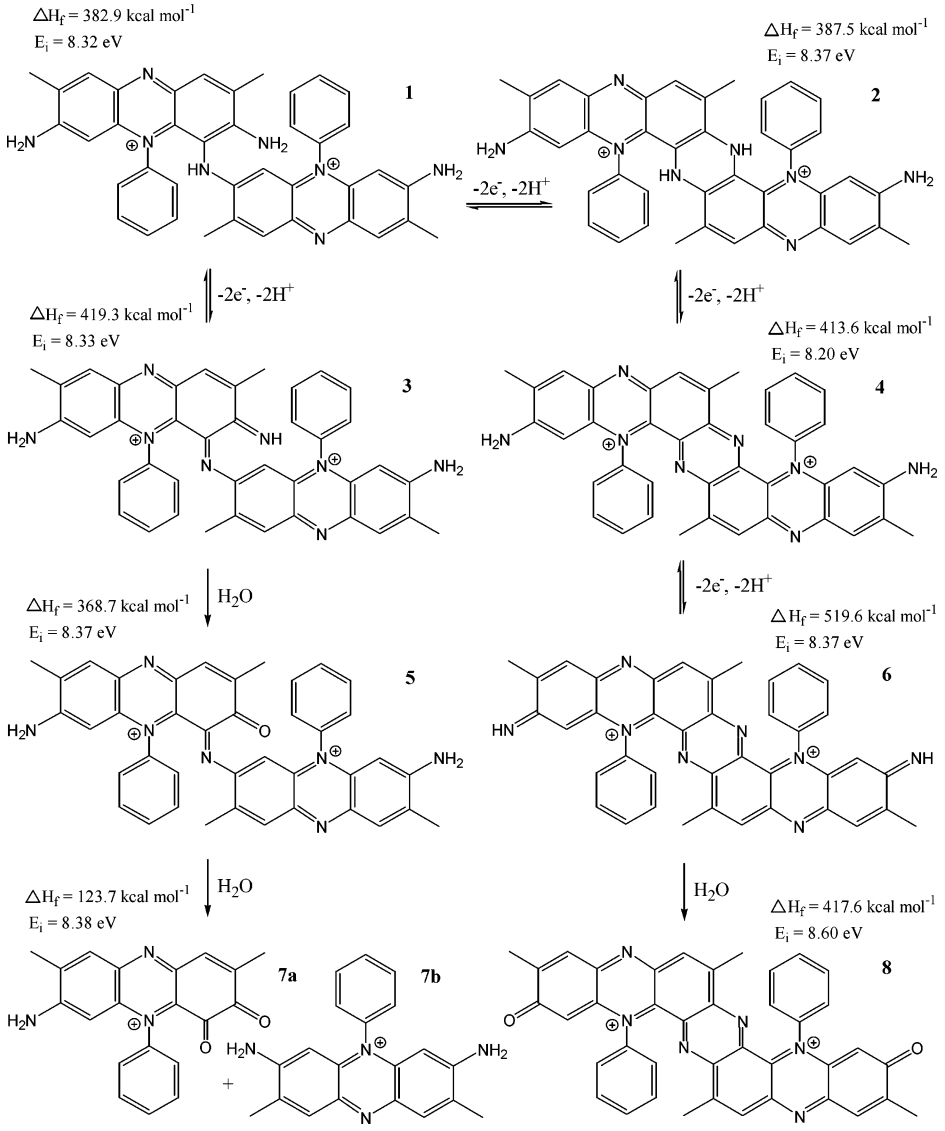

Figure 4. Redox and hydrolytic reactions of the N−C4 safranine dimer dication. MNDO-PM3-calculated E_i and ΔH_f of the hydrated N−C4 safranine dimer dication and species obtained by these reactions are shown.

free N−H stretching absorption of primary amino groups and strong, broad bands at 3306 and ∼3090 cm^{-1} due to the stretching vibrations of N−H bonds involved in hydrogen bonding.[42,46,48] The different types of intra- and intermolecular hydrogen-bonded N−H stretching vibrations are also revealed in the polymeric products by strong broad bands at 3313 and ∼3129/3063 cm^{-1} for the base form and at 3295 and ∼3126/3051 cm^{-1} for the salt form of PPSF. The contribution of various aromatic C−H stretching modes at about 3050 cm^{-1} is also possible. The transformation of monomer bands at 3443 and 3379 cm^{-1} to the one more distinct band at 3432 cm^{-1} for the base and at 3420 cm^{-1} for the salt form of PPSF, indicates formation of new secondary amino and/or imino groups in the polymer.

Polysafranine. The assignments of the main bands present in the FTIR spectra of the safranine monomer and PSF base and salt forms (Figure 7) are given in Table 4. The very strong bands due to C═C aromatic ring-stretching vibrations[17,41,42] are observed at 1607, 1529, and 1486 cm^{-1} in the FTIR spectrum of safranine, at 1609, 1530, and 1487 cm^{-1} in the spectrum of the PSF salt form, as well as at 1609, 1529, and 1486 cm^{-1} in the spectrum of the PSF base. The band at 1644 cm^{-1} in the spectrum of safranine is red-shifted to 1638 and 1636 cm^{-1} in the spectra of the PSF base and salt, respectively. As a difference from PPSF, the bands due to C═O stretching are not clearly visible in PSF spectra, indicating the reduced effect of hydrolysis on safranine polymerization in comparison with that of phenosafranine. The band due to asymmetric bending of the methyl group[45] is observed at 1453 cm^{-1} in safranine and PSF spectra with similar intensity, revealing that this group does not participate in the polymerization process. The absorption peak and the shoulder, assigned to the phenazine ring-stretching mode,[43] are observed at ∼1420 cm^{-1} in the spectra of safranine and PSF, respectively. The band attributable to phenazine ring-stretching[43] mixed with symmetric bending of the methyl group[45] is found at 1370 cm^{-1} in the monomer spectrum. This band shows a blue shift to ∼1380 cm^{-1} in the spectra of PSF samples due to the change of the nature of the ring to which the methyl group is attached.

The new peaks at 1333 and 1338 cm^{-1} in the spectra of PSF base and salt form, respectively, are attributable to the stretching vibrations of newly formed C−N bonds between linked safranine units. These peaks are assigned to the C−N bond in secondary aromatic amines,[42] and the band at 1338 cm^{-1} may also indicate the formation of structures having C−N bonds of intermediate order.[49] Bands at 1323, 1292, and 1251 cm^{-1} are

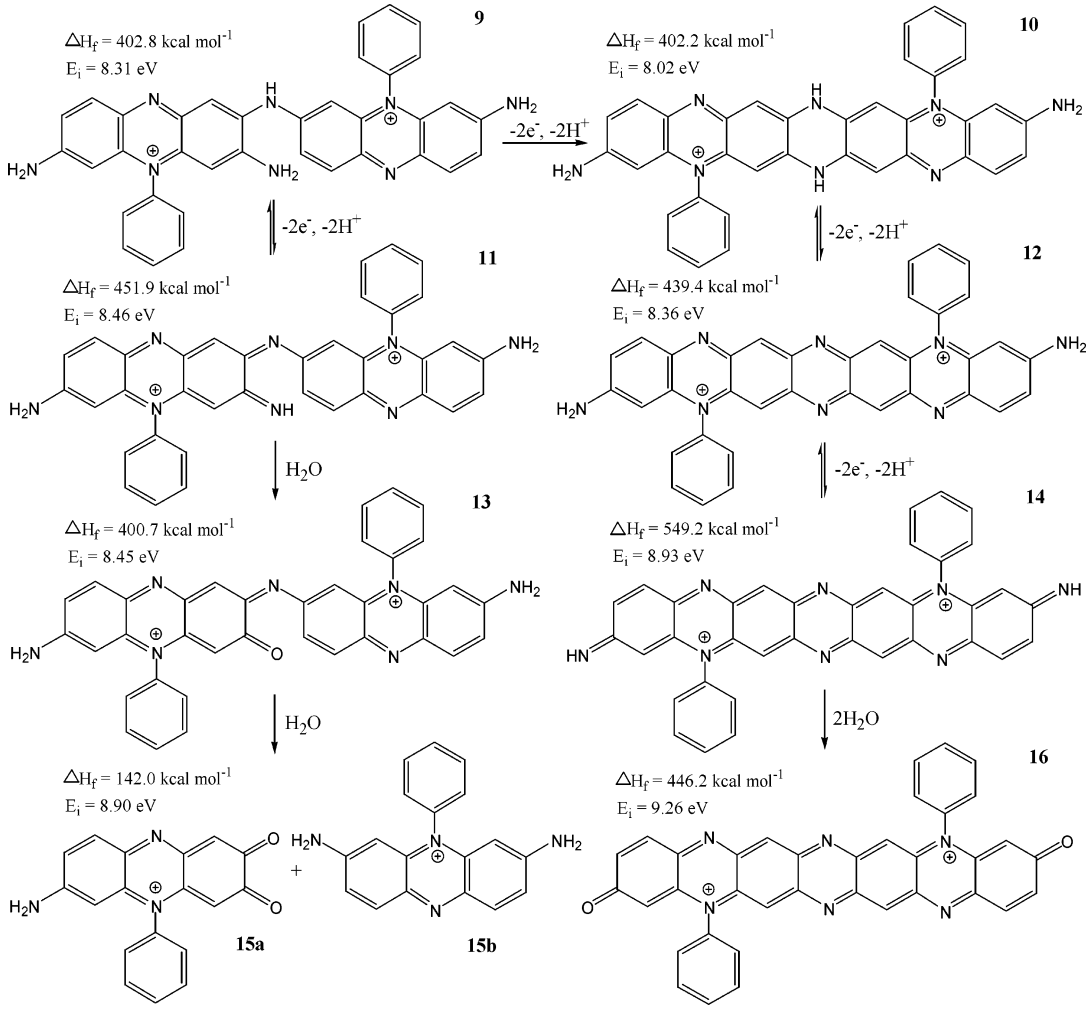

Figure 5. Redox and hydrolytic reactions of the N−C2 phenosafranine dimer dication. MNDO-PM3-calculated E_i and ΔH_f of hydrated N−C2 phenosafranine dimer dication and species obtained by these reactions are shown.

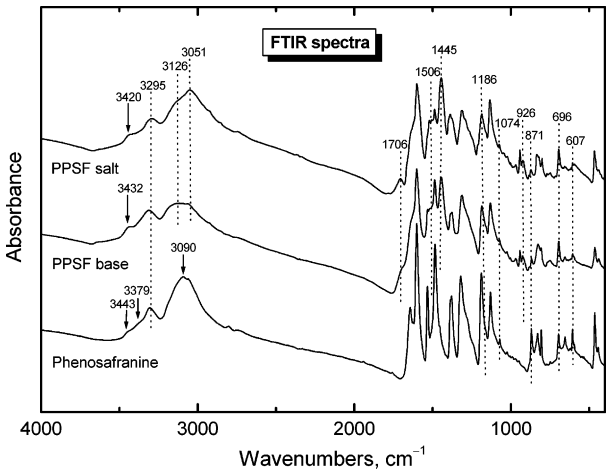

Figure 6. FTIR spectra of phenosafranine and PPSF base and salt forms.

observed in the monomer spectrum. The band at 1251 cm^{-1}, corresponding to the C−N stretching vibration of primary aromatic amines,[46] is retained with diminished intensity in the spectra of PSF, suggesting the presence of free NH_2 groups in the chains. This feature, together with the absence of new bands, which could be related to the formation of new pyrazine rings between safranine units, indicates the prevalence of ring-opened structures over ladder segments in the PSF chains. The strong bands at 1323 and 1292 cm^{-1}, due to C−N stretching, are shifted to higher frequencies: 1325/1333 (doublet) and 1296 cm^{-1} for the base form and 1326/1338 (doublet) and 1303 cm^{-1} for the salt form of PSF.

Besides the strong band that is present at ∼1190 cm^{-1} in all the analyzed spectra, a new strong one appears at 1165 cm^{-1} in the PSF spectra with respect to the monomer spectrum, indicating changes in the substitution pattern on the aromatic rings during the polymerization. These bands are assigned to aromatic δ(C−H) vibrations.[42,45,46]

The presence of the 1,2,4,5-tetrasubstituted fused benzene rings in the safranine monomer is revealed by the 877 and 901 cm^{-1} bands, assigned to γ(C−H) vibrations (1H).[42,45,46] It is difficult to recognize the pentasubstituted pattern in the presence of the 1,2,4,5-tetrasubstituted one because of their co-incident frequency region for γ(C−H) vibrations. Transformation of the 1,2,4,5-tetrasubstitution pattern to a pentasubstitution pattern during polymerization is revealed by the diminished intensity and blue shift of these bands to ∼880 and 908 cm^{-1} in the spectra of both the base and salt forms of PSF, relative to the monomer spectrum.[45,46] Similarly to PPSF, monosubstituted benzene rings of safranine are not seen to be involved in the polymerization reaction, because the PSF spectra exhibit bands characteristic of a monosubstituted ring at 1073, ∼695, and 613 cm^{-1}.

The presence of significant hydrogen bonding in PSF is indicated by broad bands at 3308 and ∼3111/3065 cm^{-1} for the base form and at 3309 and ∼3112/3061 cm^{-1} for the salt

TABLE 3: Main FTIR Bands of PPSF Base and Salt Forms and Phenosafranine in the Frequency Region 4000−400 cm^{-1} and Their Assignments

wavenumbers,[a] cm^{-1}			
phenosafranine	PPSF base	PPSF salt	assignments[b]
3443 w			asym ν(N−H) in Ar−NH_2
	3432 m	3420 m	ν(N−H) in Ar−NH_2, Ar−NH−, and C═NH
3379 m, sh			sym ν(N−H) in Ar−NH_2
3306 s, br	3313 s, br	3295 s, br	ν(N−H) H-bonded
3090 s, br	3129/3063 s, br	3126 sh/3051 s	ν(N−H) H-bonded, ν(C−H)
	1694 sh	1706 m	ν(C═O)
1643 s	1630 sh	1630 sh	ν(C═N), ν(C═C) in Phz-type ring
1602 vs	1602 vs	1601 vs	aromatic ν(C═C), NH_2 scissoring
1533 s	1531 s	1521 s	aromatic ν(C═C)
	1512 s	1506 s	ring stretching in new Ar system in PPSF
1485 vs	1487 vs	1488 s	aromatic ν(C═C)
	1445 vs	1445 vs	ring stretching in new Ar system in PPSF
1379 s	1377 s	1388 s	ring stretching in Phz-type ring, ν(C−N)
1320 vs, 1284 sh	1313 vs	1313 s, 1292 sh	ν(C−N)
1189 vs	1186 s	1186 s	δ(C−H)
1131 s, 1072 m	1132 s, 1073 m	1135 s, 1075 m	δ(C−H)
		1047 w	sym $\nu(SO_3)$ in HSO_4^-
1025, 1005 w	1025, 1003 w	1022, 1003 w	δ(C−H)
973 w−vw	970 w	970 w−m	δ(C−H) 1,2,4-trisubst ring
	926 m, 882 w	926 m, 885 w	γ(C−H) 1,2,4,5-tetrasubst ring (1H)
870 m−s	869 w−m	871 w−m	γ(C−H) 1,2,4-trisubst ring (1H)
830 m−s	827 m−s	835 m−s	γ(C−H) 1,2,4-trisubst ring (2H)
806 m−s	807 m−s	801 m	γ(C−H) 1,2,4-trisubst ring, ring deformation (Phz-type ring)
749 w	752 w	749 w	γ(C−H) monosubst ring (5H)
696 m−s	695 m−s	695 m−s	ring bending (op) monosubst ring
607 m−s	607 m	607 m	ring bending (ip) monosubst ring, NH_2 wagging

[a] Abbreviations: ν, stretching; δ, in-plane bending; γ, out-of-plane bending; vs, very strong; s, strong; m, medium; w, weak; vw, very weak; sh, shoulder; br, broad; ip, in-plane; op, out-of-plane; sym, symmetric; asym, asymmetric; Ar, aromatic; Phz, phenazine. [b] Assignments based on refs 17 and 41−48.

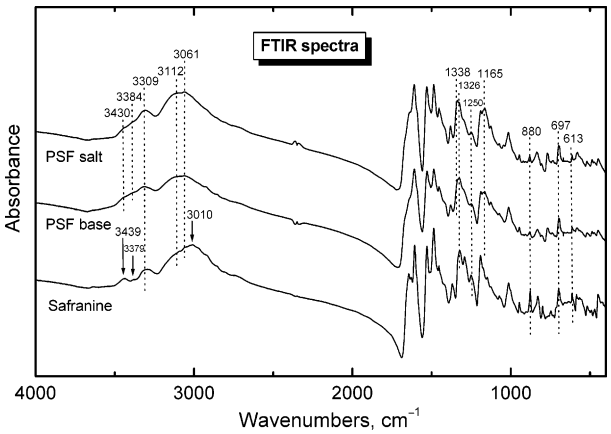

Figure 7. FTIR spectra of safranine and PSF base and salt forms.

form of PSF, due to N−H stretching vibrations, with a contribution from aromatic C−H stretching to the band at ∼3065 cm^{-1}. The formation of a new secondary amino and/or imino groups in the polymer is suggested by the appearance of the band positioned at 3387 and 3384 cm^{-1} in the spectra of the PSF base and salt form, respectively. However, the weak band at 3430 cm^{-1} (which appeared in the monomer spectrum at 3439 cm^{-1}) indicates the presence of primary amino groups in the PSF chains.

Raman Spectroscopy. Safranine and phenosafranine are well-known fluorescent dyes. For PSF and PPSF, the fluorescence is present too, which manifests itself through the shape of their Raman spectra, i.e., by the steep sloping of baselines (Figures 8 and 9).

Polyphenosafranine. The observed Raman bands of phenosafranine and PPSF samples are summarized in Table 5 with their tentative assignments. New peaks appeared at ∼1609, 1565, 1391, 733 cm^{-1}, and at 1606, 1570 (shoulder), 1393, and 727 cm^{-1} in the Raman spectra of the salt and base forms of PPSF, respectively, compared with the spectrum of the monomer. The band at ∼1609 cm^{-1} may indicate formation of a new aromatic system in PPSF and can be associated with a phenazine unit[50,51] that could be formed by an intramolecular cyclization process. Additional evidence of such a process might be the appearance of a new bands at ∼1565, ∼1397−1393, and ∼730 cm^{-1},[42,45,50−52] (Table 5). These features are consistent with previous indications obtained from FTIR spectra about the presence of ladder structural segments in PPSF. The contribution of the C═C stretching vibration of the quinonoid ring to the band at 1606 cm^{-1} is possible. The band of the monomer at 1349 cm^{-1} is strengthened and blue-shifted in the PPSF spectra to ∼1354 cm^{-1} and coincides well with the 1348 cm^{-1} band that has been reported for the phenazine itself.[51] The 1355 cm^{-1} band has also been assigned to the characteristic C∼N^+ stretching mode in the doped state of polyaniline.[53] However, its position is not changed in the spectrum of PPSF after deprotonation and therefore could not be indicative of a doped state. The band observed at 604 and 608 cm^{-1} in the spectra of the base and salt forms of PPSF, respectively, is due to the in-plane ring deformation mode of phenazine,[51,54] mixed with the in-plane ring deformation mode of the monosubstituted benzene ring in phenosafranine.[42]

Polysafranine. The Raman bands of safranine and PSF samples with their tentative assignments are presented in Table 6. The bands observed at 1546, 1632, 1505, and 611 cm^{-1} in the spectrum of the monomer are strengthened and shifted to 1545 cm^{-1} in the spectra of both forms of PSF and to ∼1644/1641, 1510/1507, and 614/613 cm^{-1} in the spectra of salt/base forms of PSF, respectively. The spectrum of the PSF base contains a peak at 1592 cm^{-1}, which can be assigned to the C═C stretching vibrations of the quinonoid ring.[55] Compared

TABLE 4: Main FTIR Bands of PSF Base and Salt Forms and Safranine in the Frequency Region 4000−400 cm^{-1} and Their Assignments

wavenumbers,[a] cm^{-1}			
safranine	PSF base	PSF salt	assignments[b]
3439 m	3430 w	3430 w	asym ν(N−H) in Ar−NH_2
3379 w	3387 m, sh	3384 m, sh	sym ν(N−H) in Ar−NH_2, ν(N−H) in Ar−NH−, C═NH
3293 m−s	3308 m−s, br	3309 s, br	ν(N−H) H-bonded
3010 s, br	3111/3065 s, br	3112/3061 s, br	ν(N−H) H-bonded, ν(C−H)
1644 s	1638 sh	1636 sh	ν(C═N), ν(C═C) in Phz-type ring
1630 s, 1607 vs	1609 s	1609 vs	aromatic ν(C═C), NH_2 scissoring
1529 vs, 1486 vs	1529 vs, 1486 vs	1530 vs, 1487 s	aromatic ν(C═C)
1453 s−vs	1453 s−vs	1453 s−vs	asym CH_3 deformation
1423 sh	1417 sh	1420 sh	ring stretching in Phz-type ring
1370 m−s	1380 m−s	1381 m−s	ring stretching in Phz-type ring, sym CH_3 deformation
	1333 vs	1338 vs	ν(C−N)
1323 vs, 1292 vs	1325 vs, 1296 sh	1326 vs, 1303 sh	ν(C−N)
1251s	1251 m−s	1251 m−s	ν(C−N)
1191 vs, 1175 sh	1189 s	1190 s	δ(C−H)
1149 s	1165 s, 1149 sh	1165 s	δ(C−H)
1126 m, 1072 m	1126 m, 1073 m	1126 m, 1073 m	δ(C−H)
		1045 m	sym $\nu(SO_3)$ in HSO_4^-
1013 s	1014 s	1015 s	δ(C−H)
901 vw, 877 s	908 vw, 879 m	908 vw, 880 m	γ(C−H) 1,2,4,5-tetrasubst ring (1H), γ(C−H) pentasubst ring (1H) in PSF
829 m−s	831 m	836 m	γ(C−H)
799 m	806 w−m	806 w−m	ring deformation (Phz-type ring)
763 w	768 m	768 m	γ(C−H) monosubst ring (5H)
698 s	695 s	697 s	ring bending (op) monosubst ring
614 m−s	612 w−m	613 m	ring bending (ip) monosubst ring, NH_2 wagging

[a] Abbreviations: ν, stretching; δ, in-plane bending; γ, out-of-plane bending; vs, very strong; s, strong; m, medium; w, weak; vw, very weak; sh, shoulder; br, broad; ip, in-plane; op, out-of-plane; sym, symmetric; asym, asymmetric; Ar, aromatic; Phz, phenazine. [b] Assignments based on refs 17 and 41−49.

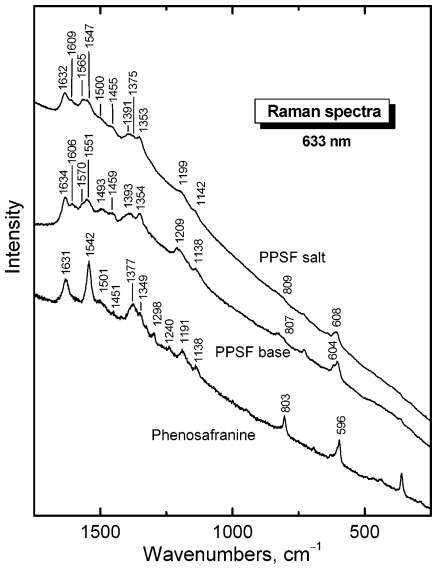

Figure 8. Raman spectra of phenosafranine and PPSF base and salt forms.

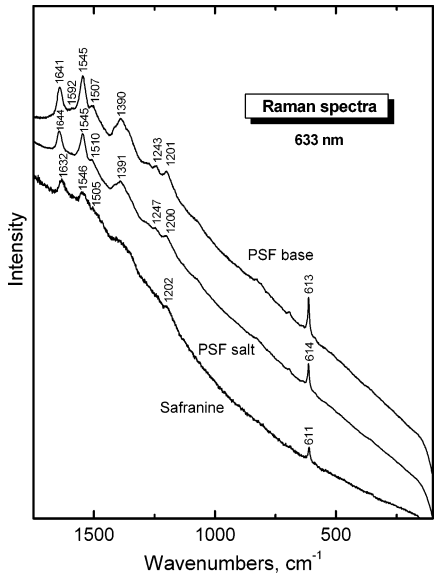

Figure 9. Raman spectra of safranine and PSF base and salt forms.

with the Raman spectrum of safranine, the spectra of PSF contain a new strong band at 1390 cm^{-1} that is attributable to a ring-stretching vibration of the phenazine ring and might indicate the formation of ladder segments. However, other indications observed in the PPSF spectrum, which could be correlated with the appearance of newly formed phenazine units, are not present in the Raman spectra of PSF. New bands, assigned to the C−N stretching vibration, are observed at 1247 and 1243 cm^{-1} in the spectra of the salt and base forms of PSF, respectively.[42,45,46]

UV−Vis Spectroscopy. Solutions of PPSF and PSF in *N*-methylpyrrolidone are red. The absorption spectra have a single peak with a maximum absorbance at 538 nm (Figure 10). The peak position is the same for both the monomers and the polymers. This means that the monomer chromophores are preserved as the main chromophores in the polymer chains. A similar observation has been found for the electrochemically synthesized PPSF, which showed an absorption maximum at the same position, ∼525 nm, as the parent monomer.[17] It should be noted that, after the oxidation, there is a marked increase in the absorbances at the tails, extending to both shorter and longer wavelengths. The similarity of UV−vis spectra of monomers and oligomers is most probably due to the significant torsion between monomeric units combined with oligomeric nature of polymerization products and the presence of relatively small content of both short-length ladder structures (predominantly ladder-structured dimeric units) and oxidized monomeric units (*ortho*-iminoquinonoid and hydrolyzed *ortho*-iminoquinonoid)

TABLE 5: Raman Bands of PPSF Base and Salt Forms and Phenosafranine in the Frequency Region 1750−250 cm^{-1} and Their Tentative Assignments (Excitation Wavelength 633 nm)

wavenumbers,[a] cm^{-1}			
phenosafranine	PPSF base	PPSF salt	tentative assignments[b]
1631	1634	1632	ring stretching
	1606	1609	ring stretching in new Ar system in PPSF, new Phz-like unit, ν(C═C)$_Q$
	1570	1565	ring stretching in new Ar system in PPSF, new Phz-like unit, ν(C═C)$_Q$
1542	1551	1547	ring stretching
1501	1493	1500	ring stretching
1451	1459	1455	ring stretching
	1393	1391	ring stretching in new Ar system in PPSF, new Phz-like unit
1377		1375	ring stretching
1349	1354	1353	ν(C−N)
1328	1327 sh		ν(C−N)
1298, 1240			ν(C−N)
1191	1209	1199	δ(C−H)
1138	1138	1142	δ(C−H)
803	807	809	ring deformation (Phz-type ring)
596	619/604	612/608	ring deformation (ip) (Phz-type ring), ring bending (ip) monosubst ring

[a] Abbreviations: ν, stretching; δ, in-plane bending; ip, in-plane; sh, shoulder; Ar, aromatic; Phz, phenazine; Q, quinonoid type ring. [b] Assignments based on refs 42, 45, 50−52, 54, and 55.

TABLE 6: Raman Bands of PSF Base and Salt Forms and Safranine in the Frequency Region 1750−250 cm^{-1} and Their Tentative Assignments (Excitation Wavelength 633 nm)

wavenumbers,[a] cm^{-1}			
safranine	PSF base	PSF salt	tentative assignments[b]
1632	1641	1644	ring stretching
	1592		ring stretching in new Ar system in PPSF, ν(C═C)$_Q$
1546	1545	1545	ring stretching
1505	1507	1510	ring stretching
1420−1340 br	1413 sh	1414 sh	ring stretching in Phz part
	1390	1391	ring stretching in new Ar system in PPSF, new Phz-like unit
	1243	1247	ν(C−N)
1202	1201	1200	δ(C−H)
611	613	614	ring deformation (ip) (Phz-type ring), ring bending (ip) monosubst ring

[a] Abbreviations: ν, stretching; δ, in-plane bending; br, broad; sh, shoulder; ip, in-plane; Ar, aromatic; Phz, phenazine; Q, quinonoid-type ring. [b] Assignments based on refs 42, 45, 46, 50−52, 54, and 55.

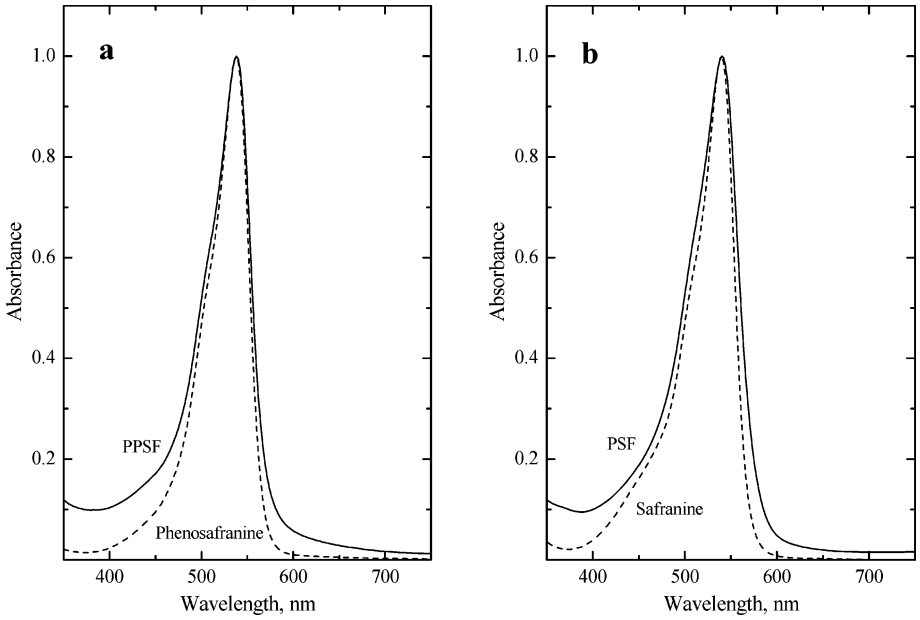

Figure 10. UV−vis spectra of (a) phenosafranine and (b) safranine (dashed lines) and of their oxidation products, PPSF and PSF (full lines), in *N*-methylpyrrolidone. The absorbances were normalized to a peak value.

in comparison with unoxidized monomeric units. This is in accordance with good solubilities of PSF and PPSF, because polymers that consist of a large amount of ladder structures should exhibit poor solubility; good solubility is expected for polymers containing a partly open ring structure, i.e., more primary amino groups.[56] It seems that planar and highly conjugated oxidized structural units represent a minor part of the investigated macromolecular structures.

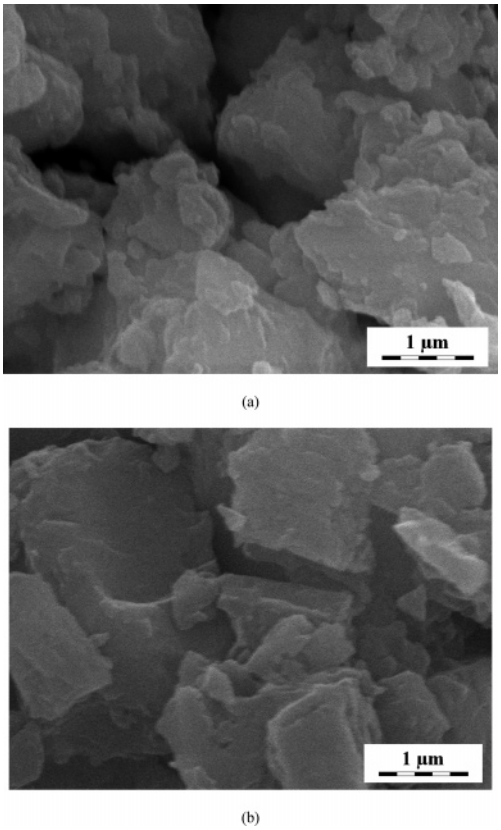

Figure 11. Scanning electron micrographs of the oxidation products of (a) phenosafranine and (b) safranine.

Morphology. The oxidation of aniline in strongly acidic media gives rise to a granular morphology of polyaniline;[55] the oxidation of aniline in water or in mildly acidic media yields products containing nanotubes, nanorods, or nanosheets.[29,30] The oxidation products of both phenosafranine and safranine have rather featureless fragmental morphology (Figure 11), and the presence of any nanostructures has not been observed.

Conclusions

The oxidation of both phenosafranine and safranine with ammonium peroxydisulfate converts the monomer, soluble in the aqueous medium, into insoluble precipitates. These are soluble in *N*-methylpyrrolidone; the molar mass of both oxidation products is several thousands, i.e., they have an oligomeric nature rather than a polymeric nature. They are nonconducting.

Semiempirical quantum chemical MNDO-PM3 calculations showed that nitrenium dications of safranines are the main reactive species formed in the first phase of oxidative polymerization of safranines with ammonium peroxydisulfate. The computations of the heat of formation of the dimeric safranine trication intermediates have led to the conclusion that the main coupling reactions of phenosafranine are N−C2 (C8) and N−C4 (C6); N−C4 (C6) is the dominant coupling mode for safranine.

The UV−vis spectra of monomers and oxidation products are similar, suggesting that the main chromophoric structures have been preserved during the oxidation. FTIR spectroscopic analysis revealed changes in the substitution patterns on safranine and phenosafranine aromatic rings caused by polymerization, which are consistent with the main coupling modes predicted theoretically. FTIR, Raman and UV−vis spectroscopic studies indicate that PSF and PPSF contain a relatively small amount of both short-length ladder structures and oxidized monomeric units in comparison with unoxidized monomeric units.

Acknowledgment. The authors thank the Ministry of Science and Environmental Protection of Serbia (Contract 142047) and the Grant Agency of the Academy of Sciences of the Czech Republic (A4050313 and A400500504) for financial support.

References and Notes

(1) Li, X.-G.; Huang, M.-R.; Duan, W.; Yang, Y. L. *Chem. Rev.* **2002**, *102*, 2925.
(2) Abdel-Azzem, M.; Yousef, U. S.; Pierre, G. *Eur. Polym. J.* **1998**, *34*, 819.
(3) Murphy, L. J. *Anal. Chem.* **1998**, *70*, 2928.
(4) Shan, J.; Cao, S. *Polym. Adv. Technol.* **2000**, *11*, 288.
(5) Ogura, K.; Shiigi, H.; Nakayama, M. *J. Electrochem. Soc.* **1996**, *143*, 2925.
(6) Puzari, A.; Baruah, J. B. *React. Funct. Polym.* **2001**, *47*, 147.
(7) Popok, V. N.; Karpovich, I. A.; Odzhaev, V. B.; Sviridov, D. V. *Nucl. Instrum. Methods Phys. Res., Sect. B* **1999**, *148*, 1106.
(8) Del Valle, M. A.; Silva, E. T.; Diaz, F. R.; Gargallo, L. *J. Polym. Sci., Part A: Polym. Chem.* **2000**, *38*, 1698.
(9) Xu, Q.; Xu, C.; Wang, Y.; Zhang, W.; Jin, L.; Tanaka, K.; Haraguchi, H.; Itoh, A. *Analyst* **2000**, *125*, 1453.
(10) Yano, J.; Yamasaki, S. *Synth. Met.* **1999**, *102*, 1157.
(11) Skompska, M.; Hillman, A. R. *J. Chem. Soc., Faraday Trans.* **1996**, *92*, 4101.
(12) D'Elia, L. F.; Ortiz, R. L.; Marquez, O. P.; Marquez, J.; Martinez, Y. *J. Electrochem. Soc.* **2001**, *148*, C297.
(13) Meneguzzi, A.; Pham, M. C.; Lacroix, J. C.; Piro, B.; Adenier, A.; Ferreira, C. A.; Lacaze, P. C. *J. Electrochem. Soc.* **2001**, *148*, B121.
(14) Naoi, K.; Suematsu, S.; Manago, A. *J. Electrochem. Soc.* **2000**, *147*, 420.
(15) Premasiri, A. H.; Euler, W. B. *Macromol. Chem. Phys.* **1995**, *196*, 3655.
(16) Thomas, K. A.; Euler, W. B. *J. Electroanal. Chem.* **2001**, *501*, 235.
(17) Komura, T.; Ishihara, M.; Yamaguchi, T.; Takahashi, K. *J. Electroanal. Chem.* **2000**, *493*, 84.
(18) Komura, T.; Yamaguchi, T.; Ishihara, M.; Niu, G. Y. *J. Electroanal. Chem.* **2001**, *513*, 59.
(19) Tanaka, K.; Tokuda, K.; Ohsaka, T. *J. Chem. Soc., Chem. Commun.* **1993**, *23*, 1770.
(20) Selvaraju, T.; Ramaraj, R. *Electrochem. Commun.* **2003**, *5*, 667.
(21) Ganesan, V.; Ramaraj, R. *J. Appl. Electrochem.* **2000**, *30*, 757.
(22) Guha, S. N.; Moorthy, P. N.; Mittal, J. P. *Int. J. Radiat. Appl. Instrum., Part C: Radiat. Phys. Chem.* **1992**, *39*, 183.
(23) Malik, P. K. *J. Phys. Chem. A* **2004**, *108*, 2675.
(24) Ensafi, A. A.; Abbasi, S.; Rezaei, B. *Spectrochim. Acta., Part A* **2001**, *57*, 1833.
(25) Sharma, G. D.; Gupta, S. K.; Roy, M. S. *Synth. Met.* **1997**, *88*, 57.
(26) O'Connell, E.; Waldner, K. M.; Roullier, L.; Laviron, E. *J. Electroanal. Chem.* **1984**, *162*, 77.
(27) Tabakova, N.; Petkova, N.; Stejskal, J. *J. Appl. Electrochem.* **1998**, *28*, 1083.
(28) Siling, S. A.; Shamahin, S. V.; Ronova, I. A.; Kovalevski, A. Yu.; Grachev, A. B.; Tsiganova, I. Yu.; Yuzhakov, V. I. *J. Appl. Polym. Sci.* **2001**, *80*, 398.
(29) (a) Trchová, M.; Šeděnková, I.; Konyushenko, E. N.; Stejskal, J.; Holler, P.; Ćirić-Marjanović, G. *J. Phys. Chem. B.* **2006**, *110*, 9461. (b) Ćirić-Marjanović, G.; Trchová, M.; Stejskal, J. *Collect. Czech. Chem. Commun.* **2006**, *71*, 1407.
(30) Konyushenko, E. N.; Stejskal, J.; Šeděnková, I.; Trchová, M.; Sapurina, I.; Cieslar, M.; Prokeš, J. *Polym. Int.* **2006**, *55*, 31.
(31) Dewar, M. J. S.; Thiel, W. *J. Am. Chem. Soc.* **1977**, *99*, 4899.
(32) Stewart, J. J. P. *J. Comput. Chem.* **1989**, *10*, 209.
(33) Stewart, J. J. P. *J. Comput. Chem.* **1989**, *10*, 221.
(34) Stewart, J. J. P. *J. Comput.-Aided Mol. Des.* **1990**, *4*, 1.
(35) Burkert, U.; Allinger, N. L. *Molecular Mechanics*; American Chemical Society: Washington, DC, 1982.
(36) Klamt, A.; Schüürmann, G. *J. Chem. Soc., Perkin Trans. 2* **1993**, 799.
(37) Stejskal, J.; Gilbert, R. G. *Pure Appl. Chem.* **2002**, *74*, 857.
(38) Eberson, L. *Adv. Phys. Org. Chem.* **1982**, *18*, 79.
(39) *CRC Handbook of Chemistry and Physics*, 84th ed.; Lide, D. R. Ed.; CRC Press: Boca Raton, FL, 2003; pp 1221, 1246, 1250.
(40) Hammond, G. S. *J. Am. Chem. Soc.* **1955**, *77*, 334.
(41) Chiba, K.; Ohsaka, T.; Ohnuki, Y.; Oyama, N. *J. Electroanal. Chem.* **1987**, *219*, 117.

(42) Socrates, G. In *Infrared and Raman Characteristic Group Frequencies*; Wiley: New York, 2001; pp 107−114, 115−123, 157−180.
(43) (a) Mitchell, M. B.; Smith, G. R.; Guillory, W. A. *J. Chem. Phys*. **1981**, *75*, 44. (b) Neto, N.; Ambrosino, F.; Califano, S. *Spectrochim. Acta* **1964**, *20*, 1503.
(44) Li, X.-G.; Duan, W.; Huang, M.-R.; Yang Y.-L. *J. Polym. Sci., Part A: Polym. Chem*. **2001**, *39*, 3989.
(45) Vien, D. L.; Colthup, N. B.; Fateley, W. G.; Grasselli, J. G. *The Handbook of Infrared and Raman Characteristic Frequencies of Organic Molecules*; Academic Press: San Diego, 1991; pp 155−178, 277−300.
(46) Bellamy, L. J. *The Infra-red Spectra of Complex Molecules*; Richard Clay: Bungay, Suffolk, U.K., 1962; pp 64−84, 248−261.
(47) Neoh, K. G.; Kang, E. T.; Tan, K. L. *Polymer* **1993**, *34*, 3921.
(48) (a) Šeděnková, I.; Trchová, M.; Blinova, N.; Stejskal, J. *Thin Solid Films* **2006**, *515*, 1640. (b) Ćirić-Marjanović, G.; Trchová, M.; Matějka, P.; Holler, P.; Marjanović, B.; Juranić, I. *React. Funct. Polym.* **2006**, *66*, 1670.
(49) Cotarelo, M. A.; Huerta, F.; Mallavia, R.; Morallón, E.; Vázquez, J. L. *Synth. Met*. **2006**, *156*, 51.
(50) Wu, L.-L.; Luo, J.; Lin, Z.-H. *J. Electroanal. Chem.* **1996**, *417*, 53.
(51) (a) Takahashi, M.; Goto, M.; Ito, M. *Chem. Phys. Lett.* **1985**, *121*, 458. (b) Durnick, T. J.; Wait, S. C. *J. Mol. Spectrosc.* **1972**, *42*, 211.
(52) (a) Do Nascimento, G. M.; Constantino, V. R. L.; Landers, R.; Temperini, M. L. A. *Macromolecules* **2004**, *37*, 9373. (b) Izumi, C. M. S.; Constantino, V. R. L.; Temperini, M. L. A. *J. Phys. Chem. B* **2005**, *109*, 22131.
(53) Guo, X.; Luo, K.; Shi, N. *J. Mater. Sci. Technol.* **2005**, *21*, 179.
(54) Takahashi, M.; Goto, M.; Ito, M. *J. Electroanal. Chem.* **1989**, *51*, 177.
(55) Trchová, M.; Matějka, P.; Brodinová, J.; Kalendová, A.; Prokeš, J.; Stejskal, J. *Polym. Degrad. Stab.* **2006**, *91*, 114.
(56) Li, X.-G.; Duan, W.; Huang, M.-R.; Rodriguez, L. N. J. *React. Funct. Polym.* **2005**, *62*, 261.